Loss of the retinoblastoma binding protein 2 (RBP2) histone demethylase suppresses tumorigenesis in mice lacking *Rb1* or *Men1*

Wenchu Lin[a,1], Jian Cao[b,1], Jiayun Liu[a], Michael L. Beshiri[c], Yuko Fujiwara[d], Joshua Francis[a], Andrew D. Cherniack[e], Christoph Geisen[a,f], Lauren P. Blair[b], Mike R. Zou[b], Xiaohua Shen[d], Dan Kawamori[g], Zongzhi Liu[b], Chiara Grisanzio[a,h], Hideo Watanabe[a], Yoji Andrew Minamishima[a], Qing Zhang[a], Rohit N. Kulkarni[g], Sabina Signoretti[a,h], Scott J. Rodig[h], Roderick T. Bronson[i], Stuart H. Orkin[d,f,j], David P. Tuck[b], Elizaveta V. Benevolenskaya[c], Matthew Meyerson[a,e,k,2], William G. Kaelin, Jr.[a,f,2], and Qin Yan[b]

[a]Department of Medical Oncology, Dana–Farber Cancer Institute and Brigham and Women's Hospital, Harvard Medical School, Boston, MA 02115; [b]Department of Pathology, Yale University School of Medicine, New Haven, CT 06520; [c]Department of Biochemistry and Molecular Genetics, University of Illinois, Chicago, IL 60607; [d]Department of Pediatric Oncology, Dana–Farber Cancer Institute and Children's Hospital, Harvard Medical School, Boston, MA 02115; [e]Broad Institute of Harvard and Massachusetts Institute of Technology, Cambridge, MA 02142; [f]Howard Hughes Medical Institute, Chevy Chase, MD 20815; [g]Section of Islet Cell and Regenerative Medicine, Department of Medicine, Joslin Diabetes Center, Harvard Medical School, Boston, MA 02115; [h]Department of Pathology, Brigham and Women's Hospital, Harvard Medical School, Boston, MA 02115; [i]Rodent Histopathology Core, Department of Pathology, Harvard Medical School, Boston, MA 02115; [j]Harvard Stem Cell Institute, Boston, MA 02115; and [k]Center for Cancer Genome Discovery, Dana-Farber Cancer Institute, Boston, MA 02115

This contribution is part of the special series of Inaugural Articles by members of the National Academy of Sciences elected in 2010.

Contributed by William G. Kaelin, June 24, 2011 (sent for review May 2, 2011)

Aberrations in epigenetic processes, such as histone methylation, can cause cancer. Retinoblastoma binding protein 2 (RBP2; also called JARID1A or KDM5A) can demethylate tri- and dimethylated lysine 4 in histone H3, which are epigenetic marks for transcriptionally active chromatin, whereas the multiple endocrine neoplasia type 1 (MEN1) tumor suppressor promotes H3K4 methylation. Previous studies suggested that inhibition of RBP2 contributed to tumor suppression by the retinoblastoma protein (pRB). Here, we show that genetic ablation of *Rbp2* decreases tumor formation and prolongs survival in *Rb1*$^{+/-}$ mice and *Men1*-defective mice. These studies link RBP2 histone demethylase activity to tumorigenesis and nominate RBP2 as a potential target for cancer therapy.

mouse model | histone methyltransferase | chromatin modifier | neuroendocrine tumor | islet cell tumor

Epigenetic alterations, like genetic alterations, can contribute to tumor initiation and progression (1, 2). Indeed, a number of genes that play roles in chromatin modifications and hence, epigenetic regulation are mutated in human cancers, including *mixed-lineage leukemia* (*MLL1*), *multiple endocrine neoplasia type 1* (*MEN1*), and *ubiquitously transcribed tetratricopeptide repeat, X chromosome* (*UTX*) (3–6).

The retinoblastoma gene (*RB1*) tumor suppressor gene is frequently inactivated in a wide variety of cancers (7). The retinoblastoma protein (pRB) inhibits S-phase entry by repressing E2F (7). In addition, pRB promotes senescence and differentiation (8). These latter two activities track closely with the ability of pRB to bind to retinoblastoma binding protein 2 (RBP2; also called JARID1A or KDM5A) rather than to E2F (9). Moreover, RBP2 siRNA is sufficient to promote senescence and differentiation in pRB-defective tumor cells in vitro (9, 10). RBP2 is a histone demethylase capable of demethylating tri- and dimethylated lysine 4 in histone H3 (H3K4me3/2) and repressing gene expression (11–14). It is, therefore, conceivable that deregulation of RBP2 histone demethylase activity contributes to pRB-defective tumor formation.

Epigenetic changes are reversible, suggesting that inhibition of specific enzymes that regulate epigenetic marks would have antitumor effects. In fact, suberoylanilide hydroxamic acid (vorinostat), a histone deacetylase (HDAC) inhibitor, was approved for the treatment of cutaneous T-cell lymphoma (15), and two DNA methyltransferase inhibitors, 5-azacytidine (azacitidine) and 5-aza-2′-deoxycytidine (decitabine), were approved for the treatment of myelodysplastic syndrome (16, 17). RBP2 belongs to a superfamily of 2-oxoglutarate–dependent dioxygenases (18, 19), which can be inhibited with drug-like small molecules (20, 21). We, therefore, used mice carrying null or conditional *Rbp2* alleles to further explore potential roles for RBP2 in pRB-defective tumorigenesis. In addition, we tested the hypothesis that loss of RBP2 H3K4 demethylase activity would inhibit tumors driven by loss of the MEN1 tumor suppressor, which is part of an H3K4 methyltransferase complex (6, 22, 23).

Results

Loss of RBP2 Inhibits Proliferation and Induces Senescence. Mouse embryonic fibroblasts (MEFs) derived from *Rbp2*$^{-/-}$ embryos on a pure genetic background proliferated more slowly than MEFs derived from WT littermate controls, especially when examined at later passages (Fig. 1 *A* and *B*). Senescence-associated β-galactosidase (SABG) staining revealed increased staining of late-passage *Rbp2*$^{-/-}$ MEFs compared with WT control MEFs (Fig. 1 *C* and *D*), suggesting that RBP2 loss promotes senescence.

To study the effect of acute RBP2 inactivation, we created mice that carry a conditional (floxed or f) *Rbp2* allele (11) and a transgene encoding a Cre-ER fusion protein, which can be activated by tamoxifen (24). Treatment of *Rbp2*$^{f/f}$*;Cre-ER* MEFs with tamoxifen led to growth arrest, but treatment of *Rbp2*$^{+/+}$*; Cre-ER* control MEFs did not lead to growth arrest (Fig. 1 *E* and *F*). Similar results were obtained when RBP2 was acutely deleted in *Rbp2*$^{f/f}$ MEFs using a retroviral vector encoding Cre recombinase (Fig. S1 *A* and *B*). Collectively, these results support the earlier conclusion, obtained with siRNAs, that RBP2 loss impairs proliferation and promotes senescence.

Author contributions: W.L., J.C., E.V.B., M.M., W.G.K., and Q.Y. designed research; W.L., J.C., J.L., M.L.B., Y.F., J.F., A.D.C., C. Geisen, L.P.B., M.R.Z., X.S., D.K., Z.L., C. Grisanzio, H.W., Y.A.M., Q.Z., R.N.K., and Q.Y. performed research; W.L., J.C., S.S., S.J.R., R.T.B., S.H.O., D.P.T., E.V.B., M.M., W.G.K., and Q.Y. analyzed data; and W.L., J.C., E.V.B., M.M., W.G.K., and Q.Y. wrote the paper.

The authors declare no conflict of interest.

Data deposition: The microarray data reported in this paper have been deposited in the Gene Expression Omnibus (GEO) database, www.ncbi.nlm.nih.gov/geo (accession nos. GSE26446 and GSE26978).

[1]W.L. and J.C. contributed equally to this work.

[2]To whom correspondence may be addressed. E-mail: matthew_meyerson@dfci.harvard.edu or william_kaelin@dfci.harvard.edu.

This article contains supporting information online at www.pnas.org/lookup/suppl/doi:10.1073/pnas.1110104108/-/DCSupplemental.

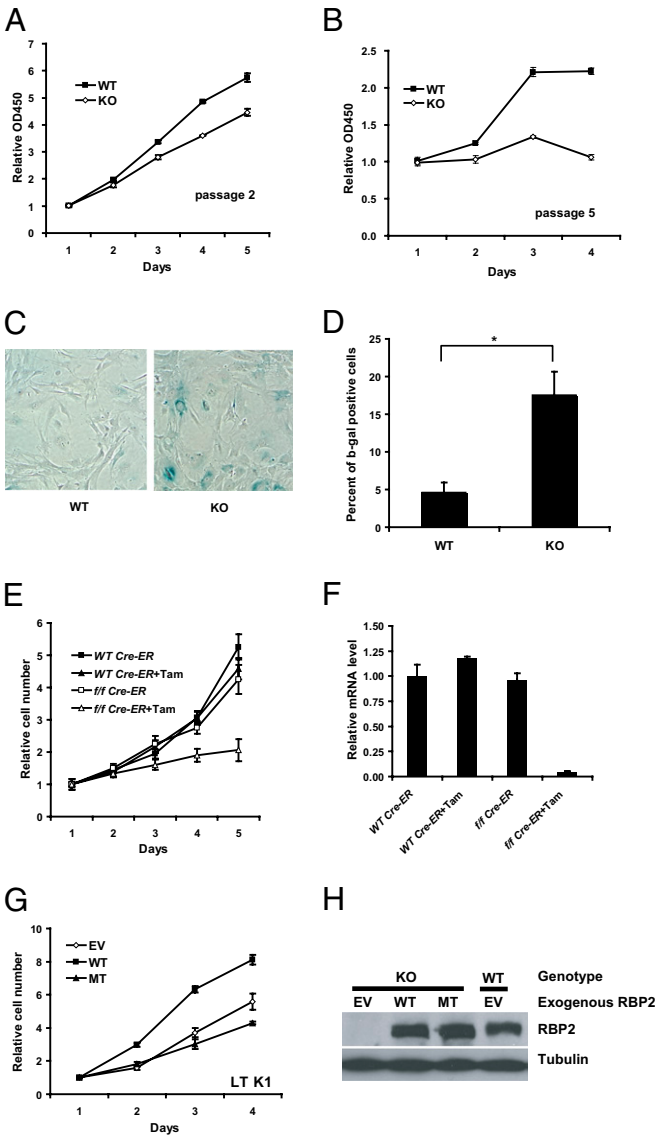

Fig. 1. Loss of RBP2 inhibits proliferation and induces senescence. (*A* and *B*) Proliferation rate of WT and *Rbp2*$^{-/-}$ (KO) primary MEFs in (*A*) early and (*B*) late passages. (*C*) Senescence-associated β-galactosidase staining of late-passage WT and *Rbp2*$^{-/-}$ MEFs. (*D*) Quantitation of β-galactosidase–positive cells of late-passage WT and *Rbp2*$^{-/-}$ MEFs from three independent experiments; 300 cells of each genotype were counted (*$P < 0.02$). (*E*) Proliferation rate of *Rbp2*$^{f/f}$*;Cre-ER* (*f/f Cre-ER*) and *Rbp2*$^{+/+}$*;Cre-ER* (*WT Cre-ER*) primary MEFs after a 6-h pulse of tamoxifen (+Tam) compared with untreated MEFs. (*F*) Real-time RT-PCR analysis of *Rbp2* in MEFs in *E*. Shown are mean values with SEM. (*G*) Proliferation rate of *Rbp2*$^{-/-}$ K1 MEFs infected with retroviruses encoding WT RBP2 (WT), RBP2 H483A (MT), or empty vector (EV). (*H*) Western blot analysis of the MEFs in *G*.

Regulation of Proliferation by RBP2 Is Dependent on Its Histone Demethylase Activity. Inactivation of p53, using either the SV40 Large T antigen (LT) K1 mutant (25) or a dominant-negative C-terminal fragment of p53 (p53^{CTF}) (26), immortalized *Rbp2*$^{-/-}$ MEFs, which was evidenced by their ability to be continually passaged in culture and absence of SABG staining; however, it did not correct their proliferation defect relative to similarly immortalized WT MEFs (Fig. S1*C* and data not shown). The availability of immortalized *Rbp2*$^{-/-}$ MEFs allowed us to ask whether the proliferation defect in *Rbp2*$^{-/-}$ cells is caused by loss of RBP2 histone demethylase activity. Reintroduction of WT RBP2, but not the histone demethylase-defective RBP2 H483A mutant (11), into LT K1-immortalized *Rbp2*$^{-/-}$ MEFs using retroviral vectors rescued the proliferation defect caused by RBP2 loss (Fig. 1 *G* and *H*).

Notably, the proliferation defect of *Rbp2*$^{-/-}$ MEFs was also rescued by inactivation of pRB, achieved with either WT LT (in contrast to LT K1) (Fig. S1*D*) or *Rb1* nullizygosity (Fig. S1 *E* and *F*). *Rbp2*$^{-/-}$*;Rb1*$^{-/-}$ primary MEFs did, however, eventually senesce, presumably because of p53 activation. Taken together, these results suggest that the senescence defect caused by RBP2 loss is p53-dependent, whereas the proliferation defect caused by RBP2 loss is pRB-dependent. Moreover, these data, together with earlier studies (9), suggest that RBP2 acts both upstream and downstream of pRB.

Loss of RBP2 Leads to Loss of Stem Cell Markers. Many developmentally important promoters contain bivalent chromatin, which consists of H3K4me3 and H3K27me3 (27). These marks ensure that the genes are poised for activation or repression on differentiation. Because RBP2 can erase H3K4me3, we asked whether loss of RBP2 affects the maintenance of mouse ES cells. We compared the gene expression profiles of *Rbp2*$^{f/f}$ and *Rbp2*$^{-/-}$ ES cells grown either in the presence of leukemia inhibitory factor (LIF) (Fig. 2*A* and *B*), which suppresses differentiation, or 6 d after LIF withdrawal (Fig. 2 *C* and *D*), which promotes differentiation, using gene set enrichment analysis (GSEA) (28). GSEA was performed using two previously defined subsets of genes: an ES genes subset that included genes that are highly expressed in undifferentiated ES cells (Fig. 2 *A* and *C*) and a differentiation genes subset that included genes that are bound by H3K27me3 and repressed in undifferentiated ES cells but activated 6 d after induction of differentiation (Fig. 2 *B* and *D*) (29). These analyses showed that loss of RBP2 down-regulates many genes that are normally highly expressed in ES cells (Fig. 2*A*) and leads to partial activation of the genes linked to differentiation (Fig. 2*B*), despite the presence of LIF, suggesting that RBP2 promotes or maintains a stem cell-like phenotype. Consistent with this idea, down-regulation of stem cell markers was more rapid in *Rbp2*$^{-/-}$ ES cells after LIF withdrawal compared with WT ES cells (Fig. 2*C*). Nonetheless, transcriptional activation of genes that are normally repressed by LIF was blunted in *Rbp2*$^{-/-}$ ES cells (Fig. 2*D*), suggesting that *Rbp2*$^{-/-}$ ES cells exit the stem cell compartment more rapidly than WT ES cells but are impaired in terms of fully executing a differentiation program.

To further examine this finding, we performed real-time PCR analysis of selected transcripts from the ES cells treated as above. In keeping with the GSEA, *Rbp2*$^{-/-}$ ES cells prematurely down-regulated the stem cell markers *Nanog* and *Oct4* in response to LIF withdrawal but failed to fully up-regulate the differentiation markers *Sox17* and *Gata6* (Fig. 2*E*). Similar findings with respect to Nanog and Oct4 were also observed when WT and *Rbp2*$^{-/-}$ ES cells were induced to form embryoid bodies (EB) and then treated with retinoic acid (RA) to promote neuronal differentiation (Fig. 2*F*). In this model, however, *Rbp2*$^{-/-}$ ES cells displayed enhanced expression of the neuronal markers Pax3 and Msi1 (Fig. 2*F*). These findings suggest that *Rbp2* deficiency down-regulates stem cell markers and promotes differentiation. Similar results were obtained with independently derived ES cell lines.

RBP2 Loss Mitigates Proliferation and Differentiation Abnormalities in pRB-Defective Cells. Down-regulation of RBP2 using siRNA inhibits the proliferation of pRB-defective tumor cells (9, 10) and restores the ability of *Rb1*$^{-/-}$ MEFs to differentiate (9). The availability of *Rbp2*$^{-/-}$ mice allowed us to address the roles of RBP2 without being confounded by siRNA-mediated off-target effects. Through appropriate crosses, we generated WT, *Rb1*$^{-/-}$, *Rbp2*$^{-/-}$, *Rbp2*$^{+/-}$*;Rb1*$^{-/-}$, and *Rbp2*$^{-/-}$*;Rb1*$^{-/-}$ embryos. Homozygous loss of *Rbp2* impaired the proliferation of *Rb1*$^{-/-}$ MEFs derived from these littermate embryos (Fig. 3*A*).

Next, WT, *Rb1*$^{-/-}$, *Rbp2*$^{-/-}$, and *Rbp2*$^{-/-}$*;Rb1*$^{-/-}$ early-passage MEFs were infected with an adenovirus-encoding MyoD and induced to differentiate in differentiation medium. RBP2 status did not influence adenoviral infection efficiency (data not shown).

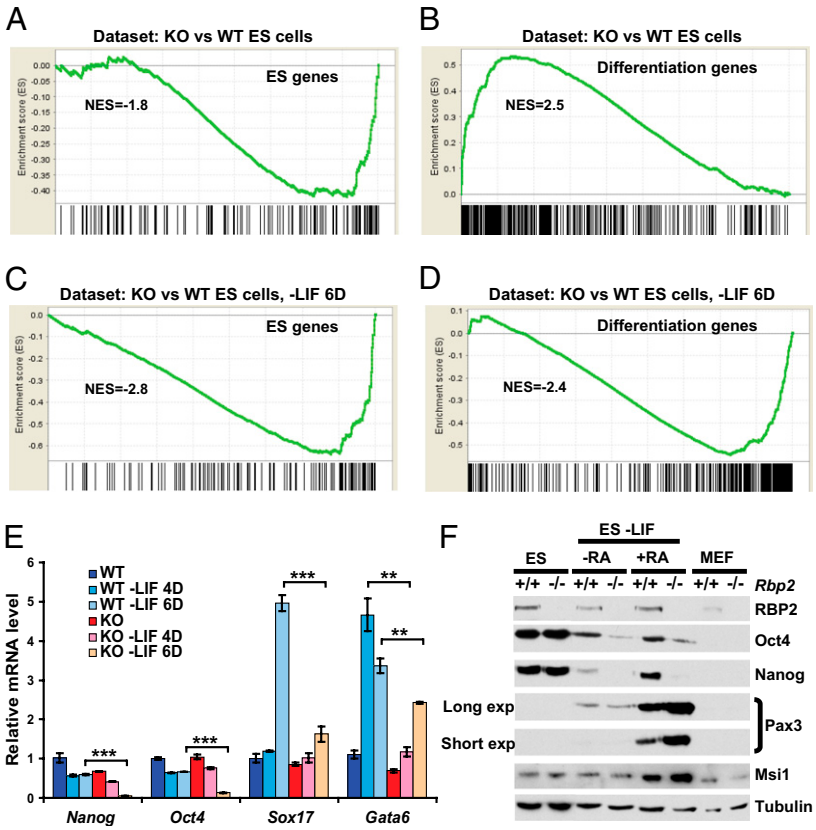

Fig. 2. Loss of RBP2 is required for maintenance and proper differentiation of mouse ES cells. (*A* and *B*) GSEA analysis of $Rbp2^{f/f}$ (WT) and $Rbp2^{-/-}$ (KO) ES cells using the gene set (*A*) highly expressed in ES cells (ES genes) or (*B*) linked to differentiation (differentiation genes). NES, normalized enrichment score. (*C* and *D*) GSEA analysis of $Rbp2^{f/f}$ (WT) and $Rbp2^{-/-}$ (KO) ES cells after induction of differentiation by 6 d of LIF withdrawal (–LIF 6D) using the gene set (*C*) highly expressed in ES cells or (*D*) linked to differentiation. (*E*) Real-time RT-PCR analysis of stem cell- and lineage-specific markers of $Rbp2^{f/f}$ (WT) and $Rbp2^{-/-}$ (KO) ES cells before and after differentiation induced by LIF withdrawal (–LIF) as in *C* and *D* for 4 (4D) or 6 d (6D; $^{**}P < 0.001$, $^{***}P < 0.0001$). (*F*) Western blot analysis of stem cell- and neuronal lineage-specific markers of WT and $Rbp2^{-/-}$ (KO) ES cells before and after differentiation in neuronal differentiation assays. RA, retinoic acid; long exp, long exposure; short exp, short exposure.

Consistent with previous studies, WT MEFs, but not $Rb1^{-/-}$ MEFs, started to form elongated myocytes 1 d after being placed in differentiation media, and they formed multinucleated myotubes shortly thereafter, which were associated with expression of the late-differentiation marker myosin heavy chain (MYHC). Loss of *Rbp2* partially rescued both MYHC expression and formation of multinucleated cells (Fig. 3 *B* and *C*). Differentiation of $Rbp2^{-/-};Rb1^{-/-}$ MEFs was also enhanced after reintroduction of WT pRB or by the pRB variant Δ663, which promotes differentiation despite an inability to bind to E2F or repress E2F-dependent promoters (8) (Fig. S2). This finding suggests that pRB has non-E2F targets in addition to RBP2 that affect differentiation.

Loss of RBP2 Suppresses Tumorigenesis Caused by Deletion of the *Rb1* or *Men1* Tumor Suppressor Genes. Although RBP2 regulates proliferation, senescence, and differentiation in vitro, which are processes deregulated in cancer, its potential relevance in transformation in vivo is unknown. We, therefore, asked whether *Rbp2* interacts genetically with *Rb1* in vivo, exploiting the fact that $Rbp2^{-/-}$ mice in a mixed genetic background are viable and have a normal lifespan (Fig. S3). $Rb1^{-/-}$ embryos die at embryonic day 14.5 (30–32), and $Rb1^{-/-}$ embryos supplied with $Rb1^{+/+}$ extraembryonic tissues die shortly after birth, possibly because of severe skeletal muscle defects (33, 34). No $Rbp2^{-/-};Rb1^{-/-}$ pups were born from $Rbp2^{+/-};Rb1^{+/-}$ intercrosses (Table S1), indicating that *Rbp2* loss cannot rescue the embryonic developmental defects caused by *Rb1* loss.

Next, we asked if loss of RBP2 would alter pRB-defective tumorigenesis. $Rb1^{+/-}$ mice develop pituitary and thyroid tumors that are associated with stochastic loss of the second *Rb1* allele (30, 35). We, therefore, examined the $Rb1^{+/-}$ progeny of matings between $Rbp2^{+/-};Rb1^{+/-}$ mice. A limited number of timed necropsies were performed on 28-wk-old mice. As expected, most (3/4) $Rb1^{+/-}$ mice had early pituitary lesions, including small tumors, whereas no abnormalities were detected in the pituitaries of all (4/4) of the $Rbp2^{-/-};Rb1^{+/-}$ mice (Fig. 4*A*), suggesting that RBP2 loss suppresses tumor initiation. The remainder of the mice were monitored and killed when they became distressed or moribund because of the development of tumors.

Importantly, deletion of *Rbp2* dramatically extended the life span of $Rb1^{+/-}$ mice (Fig. 4*B*). The median survival time improved from 47 wk for $Rbp2^{+/+};Rb1^{+/-}$ mice to 72 wk for $Rbp2^{-/-};Rb1^{+/-}$ mice. Indeed, some $Rbp2^{-/-};Rb1^{+/-}$ mice lived up to 2 y, the average life span of WT mice. Importantly, loss of one *Rbp2* allele also delayed tumorigenesis and partially extended the life span of $Rb1^{+/-}$ mice (Fig. 4*B*). Similar results were obtained when the analysis was restricted strictly to littermates (Fig. S4). Notably, all of the $Rbp2^{-/-};Rb1^{+/-}$ and $Rbp2^{+/-};Rb1^{+/-}$ mice had microscopic pituitary and/or thyroid tumors at necropsy (Table S2). This finding suggests that RBP2 delays the onset of such tumors or retards their progression rather than preventing tumor initiation.

Mammals have three RBP2 paralogs called PLU-1, SMCX, and SMCY. *Plu-1* mRNA levels were significantly increased in pituitary tumors arising in 12-mo-old $Rbp2^{-/-};Rb1^{+/-}$ mice compared with tumors arising in 12-mo-old $Rbp2^{+/+};Rb1^{+/-}$ mice (Fig. 4*C*), suggesting that compensation by Rbp2 paralogs contributes to the eventual formation of pituitary tumors in the $Rbp2^{-/-};Rb1^{+/-}$ mice.

Inactivation of the MEN1 tumor suppressor gene, like inactivation of *RB1*, leads to formation of neuroendocrine tumors (4, 36, 37). Menin, the *MEN1* gene product, is part of a complex that promotes H3K4 methylation, and this activity is diminished by tumor-associated *MEN1* mutations (6, 22, 23). We, therefore, reasoned that inactivation of the RBP2 H3K4 demethylase might partially rescue *Men1* loss. To this end, we exploited the fact that *Men1* inactivation in pancreatic islet cells leads to the development of insulinomas (37), which can be monitored based on changes in circulating insulin levels. Through appropriate matings, we generated $Men1^{f/f};Rbp2^{+/+}$, $Men1^{f/f};Rbp2^{-/-}$, and $Men1^{f/f};Rbp2^{f/f}$ mice that also expressed Cre recombinase in their pancreatic islet cells (*RIP-Cre*) (38). Inactivation of the floxed alleles

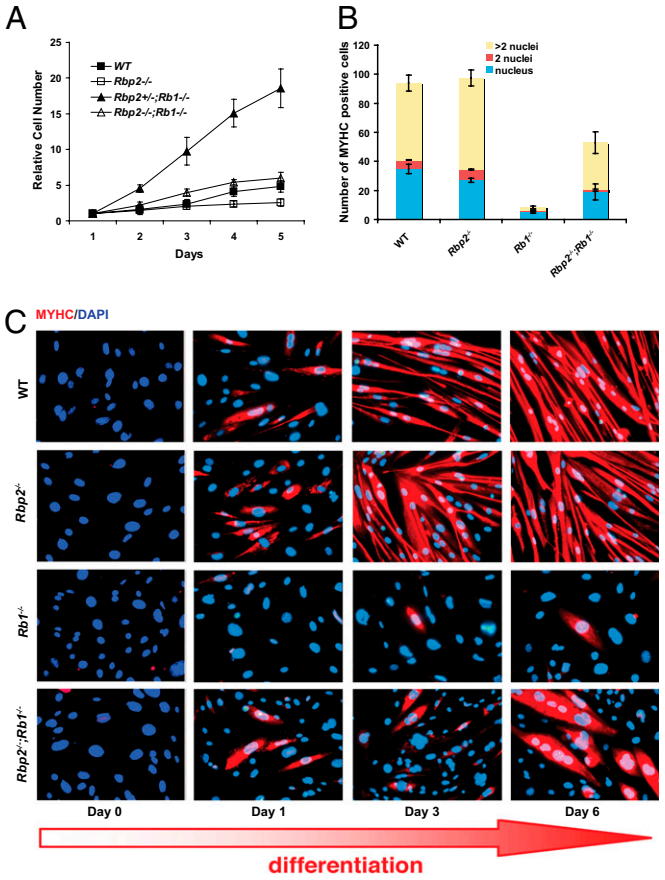

Fig. 3. Loss of RBP2 inhibits proliferation and promotes differentiation of pRB-defective cells. (*A*) Proliferation rate of WT, *Rbp2*$^{-/-}$, *Rbp2*$^{+/-}$;*Rb1*$^{-/-}$, and *Rbp2*$^{-/-}$;*Rb1*$^{-/-}$ MEFs. (*B*) Quantitation of MYHC-positive cells in five representative fields at day 6 of myogenic differentiation. MEFs of the indicated genotypes were infected with an adenovirus expressing MyoD to induce myogenic differentiation. The MYHC-positive cells were also scored for the presence of multiple nuclei. Shown are mean values with SEM from three independent experiments. (*C*) MYHC expression in MEFs during myogenic differentiation. The cells were fixed and stained with anti-MYHC antibody (red) and counterstained with the nuclear stain DAPI (blue) after growth for the indicated number of days in differentiation media.

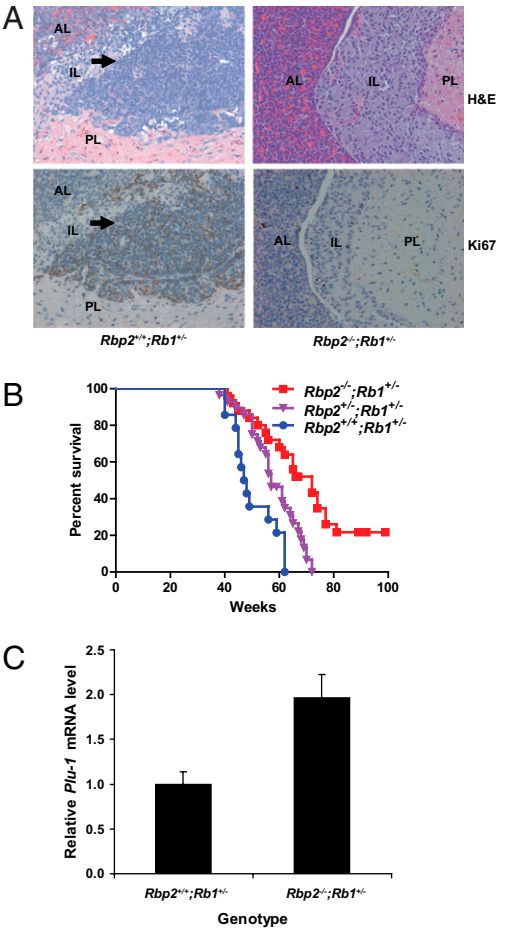

Fig. 4. Loss of RBP2 suppresses *Rb1*$^{+/-}$ tumorigenesis in vivo. (*A*) H&E staining (*Upper*) and Ki67 staining (*Lower*) of the pituitary glands of 28-wk-old *Rbp2*$^{+/+}$;*Rb1*$^{+/-}$ (*Left*) and *Rbp2*$^{-/-}$;*Rb1*$^{+/-}$ (*Right*) mice. The arrow in *Left* points to a tiny pituitary tumor in the intermediate lobe. AL, anterior lobe; IL, intermediate lobe; PL, posterior lobe. (*B*) Kaplan–Meier survival curve comparing *Rbp2*$^{+/+}$;*Rb1*$^{+/-}$ (n = 14), *Rbp2*$^{+/-}$;*Rb1*$^{+/-}$ (n = 28), and *Rbp2*$^{-/-}$;*Rb1*$^{+/-}$ (n = 24) mice ($P <$ 0.0001 for *Rbp2*$^{-/-}$;*Rb1*$^{+/-}$ vs. *Rbp2*$^{+/+}$;*Rb1*$^{+/-}$ and $P < 0.01$ for *Rbp2*$^{+/-}$;*Rb1*$^{+/-}$ vs. *Rbp2*$^{+/+}$;*Rb1*$^{+/-}$). (*C*) Real-time RT-PCR analysis of *Plu-1* mRNA in pituitary tumors from 12-mo-old *Rbp2*$^{-/-}$;*Rb1*$^{+/-}$ (n = 4) and *Rbp2*$^{+/+}$;*Rb1*$^{+/-}$ (n = 2) mice. Shown are mean values with SEM.

was confirmed by anti-menin and anti-RBP2 immunohistochemistry (Fig. S5).

Rbp2 inactivation, either systemically (Fig. 5*A*) or specifically in islet β-cells (Fig. 5*B*), substantially decreased islet cell tumor burden, which was measured by circulating insulin levels (Fig. 5*C*), and enhanced survival (Fig. 5 *A* and *B*). The median survival for *Men1*$^{f/f}$;*Rbp2*$^{+/+}$;*RIP-Cre* mice was 45 wk compared with median survivals of 68 wk for *Men1*$^{f/f}$;*Rbp2*$^{-/-}$;*RIP-Cre* mice (Fig. 5*A*) or 69 wk for *Men1*$^{f/f}$;*Rbp2*$^{f/f}$;*RIP-Cre* mice (Fig. 5*B*), respectively. Inactivation of *Rbp2* in islet cells of *Men1*$^{+/+}$ mice did not grossly affect islet histology or function, which was determined by gene expression profiling (Fig. S6), circulating insulin (Fig. 5*C*), and glucose levels (data not shown).

We also performed timed necropsies on a limited number of *Men1*$^{f/f}$;*Rbp2*$^{+/+}$;*RIP-Cre* and *Men1*$^{f/f}$;*Rbp2*$^{f/f}$;*RIP-Cre* mice (Fig. 6*A*). By 2 mo of age, 50% (5/10) of the former exhibited islet cell hyperplasia compared with zero of the latter (0/8) (Table S3). The prevalence of cellular atypia and insulinoma at 4 and 8 mo was dramatically reduced by loss of *Rbp2*. By 10 mo of age, all (15/15) of the *Men1*$^{f/f}$;*Rbp2*$^{+/+}$;*RIP-Cre* mice had insulinomas compared with 2 of 21 *Men1*$^{f/f}$;*Rbp2*$^{f/f}$;*RIP-Cre* mice (Table S3). These findings indicate that *Rbp2* loss significantly delays the onset of hyperplasia, atypia, and insulinoma in this model.

Notably, insulinomas were observed in some (2/5) 12-mo-old *Men1*$^{f/f}$;*Rbp2*$^{f/f}$;*RIP-Cre* mice at necropsy. Comparison of insulinomas from 12-mo-old *Men1*$^{f/f}$;*Rbp2*$^{f/f}$;*RIP-Cre* mice with *Men1*$^{f/f}$;*RIP-Cre* mice revealed increased expression of *Plu-1* but not *Smcx* and *Smcy* after *Rbp2* loss (Fig. 6*B*). This increase, however, was not observed in spleens from 12-mo-old *Men1*$^{f/f}$;*Rbp2*$^{f/f}$;*RIP-Cre* mice or pancreatic islets from 2-mo-old *Men1*$^{f/f}$;*Rbp2*$^{f/f}$;*RIP-Cre* mice (data not shown). These observations suggest that the eventual formation of insulinomas in *Men1*$^{f/f}$;*Rbp2*$^{f/f}$;*RIP-Cre* mice depends on increased levels of PLU-1, perhaps occurring stochastically over time.

To begin to understand the mechanisms underlying these differences, we injected 2-mo-old mice with BrdU and examined their pancreata 5 h later. As expected, BrdU incorporation was increased in the islets of *Men1*$^{f/f}$;*Rbp2*$^{+/+}$;*RIP-Cre* mice compared with WT controls (Fig. 6 *C* and *D*). This increase was not observed, however, in islets that concurrently lacked *Rbp2*. We did not observe differences in bulk H3K4 trimethylation by immunohistochemistry (data not shown), possibly reflecting the activity of additional H3K4 methyltransferases and demethylases.

To begin to assess the molecular basis for the effect of *Rbp2* loss in attenuating tumorigenesis, we performed mRNA profiling

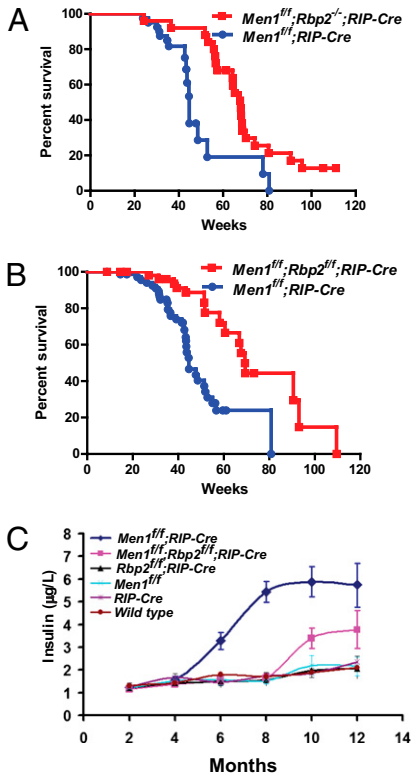

Fig. 5. Loss of RBP2 suppresses *Men1*-defective pancreatic islet cell tumorigenesis. (*A* and *B*) Kaplan–Meier survival curves comparing (*A*) *Men1*$^{f/f}$;*RIP-Cre* mice (n = 40) with *Men1*$^{f/f}$;*Rbp2*$^{-/-}$;*RIP-Cre* (n = 25; $P < 0.005$) or (*B*) *Men1*$^{f/f}$;*RIP-Cre* mice (n = 85) with *Men1*$^{f/f}$;*Rbp2*$^{f/f}$;*RIP-Cre* (n = 72; $P < 0.0001$). (*C*) Circulating insulin levels in mice with the indicated genotypes.

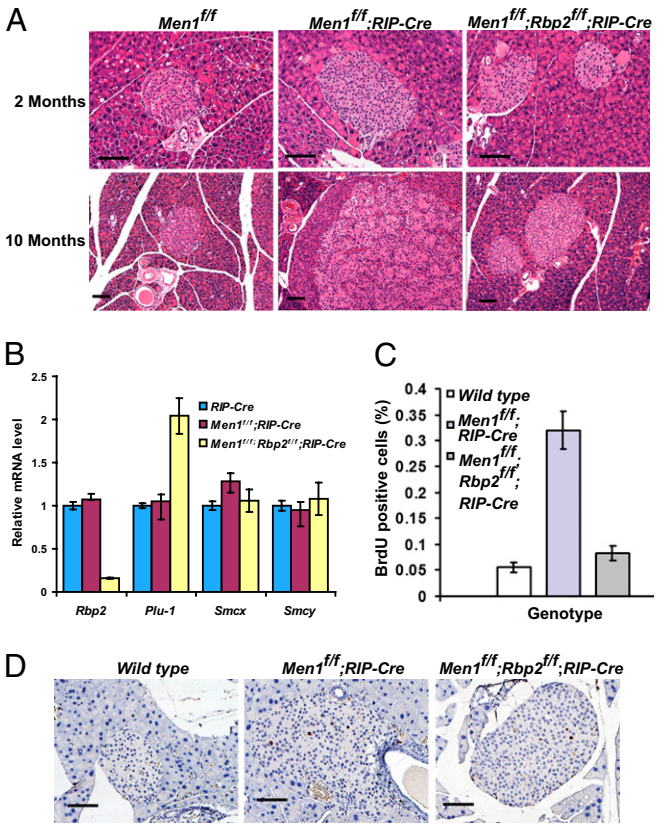

Fig. 6. RBP2 loss inhibits proliferation of *Men1*-defective islets. (*A* and *D*) Representative (*A*) H&E and (*D*) BrdU staining of pancreata from mice with the indicated genotypes. (Scale bar: 100 μm.) BrdU was administered by i.p. injection to 2-mo-old mice 5 h before sacrifice. (*B*) Real-time RT-PCR analysis of the indicated mRNAs in pancreatic islets of 12-mo-old *RIP-Cre* mice (n = 2) and pancreatic islet tumors of 12-mo-old *Men1*$^{f/f}$;*RIP-Cre* mice (n = 2) and *Men1*$^{f/f}$;*Rbp2*$^{f/f}$;*RIP-Cre* mice (n = 2). Shown are mean values with SEM. (*C*) Quantitation of the islet cell BrdU incorporation measured in *D*.

using DNA microarrays on pancreatic islets isolated from 2-mo-old WT, *RIP-Cre*, *Men1*$^{f/f}$;*RIP-Cre*, *Rbp2*$^{f/f}$;*RIP-Cre*, and *Men1*$^{f/f}$;*Rbp2*$^{f/f}$;*RIP-Cre* mice. The gene expression changes caused by deletion of *Men1* overlap with those changes reported previously (39) (Dataset S1).

To determine the effects of *Rbp2* inactivation on the gene expression changes in *Men1*-deficient islets, we compared the gene expression changes in *Men1*$^{f/f}$;*Rbp2*$^{f/f}$;*RIP-Cre*, *Men1*$^{f/f}$;*RIP-Cre*, and *Rbp2*$^{f/f}$;*RIP-Cre* islets with WT and *RIP-Cre* control islets. The effects of *Men1* deletion on pancreatic islet gene expression were reversed by *Rbp2* loss for a number of genes belonging to several classes, including genes involved in signaling, cell cycle, and apoptosis (Fig. 7 *A* and *B*). The reversal by *Rbp2* deletion of expression changes associated with *Men1* deletion in islets was confirmed by real-time RT-PCR (Fig. 7*C*).

Discussion

We confirmed that loss of RBP2 impairs proliferation, promotes senescence, and enhances differentiation in vitro. Notably, deletion of *Rbp2* was insufficient to rescue the embryonic developmental defects caused by *Rb1* loss but significantly suppressed pituitary and thyroid tumorigenesis in *Rb1*$^{+/-}$ mice and islet cell tumorigenesis after inactivation of *Men1* in pancreatic neuroendocrine cells.

The canonical pRB targets are members of the E2F transcription factor family, and suppression of E2F-responsive promoters contributes to cell-cycle control and tumor suppression by pRB (7). pRB also biochemically interacts with a number of chromatin modifiers, including HDACs (40–42), SWI/SNF chromatin remodeling complexes (43, 44), H3K9 methyltransferases Suv39h1 (45) and RIZ1 (46), H4K20 methyltransferase Suv4-20h (47), and DNA methyltransferase 1 (DNMT1) (48). Our findings, together with earlier biochemical and siRNA-derived data, suggest that another pRB-interacting chromatin modifier, RBP2, contributes to tumor suppression by pRB. RBP2 loss inhibits cell proliferation in a pRB-dependent manner, placing RBP2 upstream of pRB. However, RBP2 inhibits senescence and differentiation in pRB-defective tumor cells, and loss of RBP2 inhibits formation of pRB-defective endocrine tumors, suggesting that RBP2 also acts downstream of pRB. In summary, tumor suppression by pRB might involve coordinated regulation of both E2F and RBP2. Consistent with this idea, RBP2 is recruited to E2F target genes during differentiation (49).

It is increasingly clear that alterations in histone methylation play important roles in cancer in general (50, 51). For example, MLL1, a subunit of an H3K4 methyltransferase complex, is frequently translocated in leukemia (52, 53), whereas another H3K4 methyltransferase subunit gene, *MEN1*, is frequently mutated in endocrine tumors (4, 6, 22, 23). EZH2, the catalytic subunit of an H3K27 methyltransferase polycomb repressive complex 2, is overexpressed in aggressive prostate cancers (54). Finally, copy number changes and intragenic mutations affecting histone methyltransferses and demethylases, such as the UTX H3K27 histone demethylase, are increasingly being identified in cancers (5, 55, 56).

RBP2 is one of four proteins [together with PLU-1 (also known as KDM5B or JARID1B), SMCX (also known as KDM5C or JARID1C), and SMCY (also known as KDM5D or JARID1D)] capable of demethylating trimethylated H3K4 (57). This mark is usually associated with actively transcribed genes and is also found at bivalent domains in association with trimethylated H3K27, which is usually linked to transcriptional repression (27).

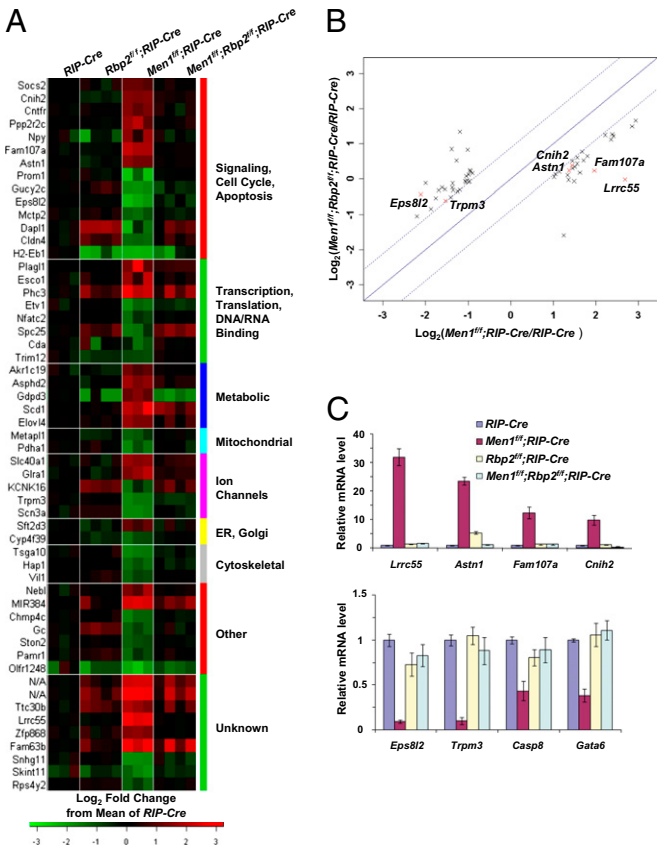

Fig. 7. *Rbp2* loss reverses gene expression changes caused by *Men1* loss. (*A* and *B*) Microarray data of transcripts that are significantly altered (*t* test, $P < 0.05$; fold change > 1.85) in islets from *Men1*$^{f/f}$;*RIP-Cre* mice compared with islets from *RIP-Cre* control mice and *Men1*$^{f/f}$;*Rbp2*$^{f/f}$;*RIP-Cre* mice. (*A*) Heat map representing relative transcript abundance for the indicated genes (rows) and islet preparations from individual mice (columns). The color scale is based on $\log_2$ fold change from the mean signal in *RIP-Cre* mouse islets. (*B*) Scatter plot depicting the average fold change of expression of these transcripts in islets from the indicated KO mice compared with *RIP-Cre* mice. (*C*) Real-time RT-PCR analysis of the genes marked by red crosses in *B* and *Casp8* and *Gata6*. Shown are mean values with SEM from at least triplicate experiments.

The paradoxical co-association of both an activating and repressive methylation mark is thought to poise genes to respond to either inhibitory or stimulatory signals linked to differentiation and control of cell fate. Consistent with this idea, bivalent domains seem to be important for both stem cell and cancer biology.

Interestingly, RBP2 has been reported to be translocated in leukemia (58, 59) and overexpressed in gastric cancer (10). A recent study suggested that increased expression of RBP2 promoted a more stem-like phenotype, consistent with our results, and enhanced resistance to anticancer agents (60). PLU-1 is overexpressed in breast (61) and prostate cancers (62), and shRNA-mediated down-regulation of PLU-1 suppresses breast cancer growth in a syngeneic mouse cancer model (63). Interestingly, PLU-1 marks a subpopulation of slow-cycling melanoma cells required for continuous tumor growth (64), and its overexpression in ES cells suppresses differentiation (65). Therefore, PLU-1, like RBP2, might maintain a stem-like phenotype and promote tumorigenesis. Finally, SMCX was recently found to be mutated in a subset of clear cell renal cell carcinomas (5).

Both *RB1* and *MEN1* have been linked to neuroendocrine tumors. The former is linked to pituitary and thyroid tumors in mice (30, 35) and small cell lung cancer in man (66), whereas the latter is linked to pituitary, parathyroid, and pancreatic islet cell tumors in both species (4, 36, 37). Interestingly, inactivation of *Rb1* and *Men1* in neuroendocrine tumors arising in *Rb1*$^{+/-}$; *Men1*$^{+/-}$ compound heterozygous mice is mutually exclusive (67, 68), suggesting that *Rb1* and *Men1* share a critical activity or activities relevant to neuroendocrine tumorigenesis. Our studies suggest that regulation of H3K4 methylation is one such activity.

Enzymes have historically proven to be tractable drug targets. RBP2 and its paralogs PLU-1, SMCX, and SMCY are 2-oxoglutarate–dependent dioxygenases (18, 19). These enzymes can be inhibited with drug-like small organic molecules that act competitively with respect to 2-oxoglutarate, interfere with iron use, or both (20, 21). Our findings suggest that RBP2-inhibitory drugs, should they be developed, would have anticancer activity. Furthermore, elevated expression of PLU-1 in *Rbp2* null tumors (Fig. 4*C* and 6*B*) suggests that RBP2 inhibitors that also inhibit PLU-1, if they were safe, would be more effective than inhibitors that target RBP2 alone.

Materials and Methods

Mouse Experiments. *Rbp2*$^{-/-}$ and *Rbp2*$^{f/f}$ mice were described previously (11) and backcrossed to C57BL/6 strain for at least five generations. *Rbp2*$^{+/-}$ mice were intercrossed to generate *Rbp2*$^{-/-}$ MEFs and WT littermate control MEFs. *Rbp2*$^{f/f}$ mice were crossed with C57BL/6 chicken β-actin *Cre-ER* mice (24, 69) to obtain *Rbp2*$^{+/f}$;*Cre-ER* mice. *Rbp2*$^{+/f}$;*Cre-ER* mice were crossed with *Rbp2*$^{+/f}$ mice to generate *Rbp2*$^{f/f}$;*Cre-ER* MEFs and *Rbp2*$^{+/+}$;*Cre-ER* littermate control MEFs. *Rb1*$^{+/-}$ mice on a C57BL/6 background (30) were obtained from the National Cancer Institute Mouse Repository. *Rb1*$^{+/-}$ mice were crossed with *Rbp2*$^{-/-}$ mice on a mixed 129/SvEv, FVB/N, and C57BL/6 background to obtain *Rbp2*$^{+/-}$;*Rb1*$^{+/-}$ mice. These mice were then intercrossed to generate the experimental cohorts of *Rb1*$^{+/-}$, *Rbp2*$^{+/-}$;*Rb1*$^{+/-}$ and *Rbp2*$^{-/-}$;*Rb1*$^{+/-}$ mice.

Men1 conditional KO mice were described previously (6) and maintained on a mixed 129s6, FVB/N, and C57BL/6 background. To specifically delete the *Men1* gene in pancreatic islet β-cells, *Men1*$^{f/f}$ mice were crossed with *RIP-Cre* transgenic mice (38). The *Men1*$^{+/f}$;*RIP-Cre* mice were crossed with *Men1*$^{+/f}$ mice to generate *Men1*$^{f/f}$;*RIP-Cre* mice. *Men1*$^{f/f}$;*Rbp2*$^{-/-}$;*RIP-Cre* and *Men1*$^{f/f}$;*Rbp2*$^{f/f}$;*RIP-Cre* mice were generated by introducing *Rbp2* null and floxed alleles into the *Men1*$^{f/f}$;*RIP-Cre* mice through appropriate matings. For in vitro proliferation and differentiation assays, *Rb1*$^{+/-}$ mice were crossed with *Rbp2*$^{+/-}$ mice on a pure C57BL/6 background to obtain *Rbp2*$^{+/-}$;*Rb1*$^{+/-}$ mice, which were intercrossed to generate WT, *Rbp2*$^{-/-}$, *Rb1*$^{-/-}$, *Rbp2*$^{+/-}$;*Rb1*$^{-/-}$, and *Rbp2*$^{-/-}$;*Rb1*$^{-/-}$ MEFs. Mice and cells carrying *Men1* floxed alleles were genotyped using primers described in *SI Materials and Methods*, and all other mice and cells were genotyped as described (11, 24, 30, 38). All mice were maintained in the research animal facility of the Dana–Farber Cancer Institute and Yale Animal Resources Center in accordance with the National Institutes of Health guidelines. All procedures involving mice were approved by the Institutional Animal Care and Use Committees of the Dana–Farber Cancer Institute and Yale University.

ES Cell Culture and Differentiation. In Fig. 2 *A–E*, *Rbp2*$^{f/f}$ ES cells were isolated from mouse blastocysts after intercrossing *Rbp2*$^{f/f}$ mice on a pure C57BL/6 background and transiently transfected with pBS500/EF1α-GFPCre plasmid. GFP-positive cells were isolated by FACS and plated at low density. Isolated colonies were then expanded into ES lines. Successful recombination of the *Rbp2* locus was confirmed by PCR and Western blot analysis. In Fig. 2*F*, WT and *Rbp2*$^{-/-}$ ES cells were isolated from mouse blastocysts after intercrossing *Rbp2*$^{+/-}$ mice. WT, *Rbp2*$^{f/f}$, and *Rbp2*$^{-/-}$ ES cells were maintained on mitomycin C-treated MEF feeders in standard ES medium: DMEM containing 15% heat-inactivated FBS, 0.1 mM 2-mercaptoethanol, 2 mM L-glutamine, 0.1 mM nonessential amino acid, 1% Embryomax ES cell-qualified nucleosides (100× stock; Chemicon), 1,000 U/mL recombinant LIF (Chemicon), 50 U/mL penicillin/streptomycin.

For differentiation assays, ES cells were passaged at least three times without feeders and maintained on gelatin-coated plates in standard ES culture medium containing LIF. In Fig. 2 *A–E*, the ES cells were induced to differentiate by removing LIF from culture medium and were harvested at 4 or 6 d after differentiation for analysis. In Fig. 2*F*, ES cells were induced to differentiate on untreated plates to form EB for 2 d, and were then treated with 1 μM retinoic acid to induce neuronal differentiation for 3 d. After 2 more days on untreated plates, the cells were plated onto gelatin-coated plates and grown for an additional 4 d before Western blot analysis.

Gene Expression Profiling. Subconfluent *Rbp2*$^{f/f}$ and *Rbp2*$^{-/-}$ ES cells were harvested for RNA isolation using the RNeasy mini kit with on-column DNase

digestion (Qiagen). Gene expression profiling was performed using Affymetrix GeneChip mouse genome 430 2.0 arrays. Raw gene expression profiling data were analyzed using dChip (70). The two gene sets used for gene set enrichment analysis were described previously (29). The differentiation genes include all genes that are marked by both H3K27me3 and EZH1 in WT ES cells and up-regulated at least threefold 6 d after induction of differentiation by LIF withdrawal. The ES genes are genes highly expressed in pluripotent ES cells compared with differentiated cells.

Pancreatic islets were isolated as described (71). Briefly, 0.25 mg/mL Liberase solution (Roche) in serum-free M199 medium were injected into pancreata through the common bile duct of anesthetized 2-mo-old male mice. The inflated pancreata were incubated at 37 °C for 20 min for digestion before filtered through mesh. Then, islets were purified through histopaque gradient purification and gravity sedimentation. Finally, islets were hand-picked from dark field dishes under a dissecting microscope for RNA isolation using the RNeasy mini kit (Qiagen). Islet RNAs were expression-profiled on Affymetrix GeneChip Mouse Gene 1.0 ST arrays. Raw gene expression profiling data were analyzed using dChip (70). Transcripts were defined to be significantly changed based on a *t* test $P < 0.05$. The expression data reported in this paper have been deposited in the National Center for Biotechnology Information Gene Expression Omnibus database under accession numbers GSE26446 and GSE26978.

ACKNOWLEDGMENTS. We thank members of the E.V.B., W.G.K., M.M., S.H.O., and Q.Y. laboratories for their kind help and valuable discussions. We thank Dr. Lili Yamasaki for her valuable comments. We also thank the laboratory members of Dr. David Stern for their kind help. We thank Dr. Ronald DePinho for providing *Cre-ER* transgenic mice and Dr. Seung Kim for providing *RIP-Cre* mice. We thank Dr. Edward Fox and the Dana–Farber Cancer Institute microarray core facility and Yale Center for Genome Analysis for gene expression profiling studies. We also thank Harvard rodent histology core, Harvard specialized histopathololgy core, Dr. Alexander Vortmeyer, and the Yale research histology facility for histological analysis. This work was supported by National Institutes of Health Grants CA138631 (to E.V.B.), CA076120 (to W.G.K.), and CA16359 (to Yale Comprehensive Cancer Center), the Raymond and Beverly Sackler Fund for the Arts and Sciences (M.M.), the Caring for Carcinoid Foundation (M.M), and the V Scholar Award (to Q.Y.). W.G.K. is a Howard Hughes Medical Institute Investigator and a Doris Duke Distinguished Scientist. Q.Y. is a Breast Cancer Alliance Young Investigator and an Alexander and Margaret Stewart Trust Fellow.

1. Feinberg AP, Ohlsson R, Henikoff S (2006) The epigenetic progenitor origin of human cancer. *Nat Rev Genet* 7:21–33.
2. Esteller M (2008) Epigenetics in cancer. *N Engl J Med* 358:1148–1159.
3. Rowley JD (1993) Rearrangements involving chromosome band 11Q23 in acute leukaemia. *Semin Cancer Biol* 4:377–385.
4. Chandrasekharappa SC, et al. (1997) Positional cloning of the gene for multiple endocrine neoplasia-type 1. *Science* 276:404–407.
5. Dalgliesh GL, et al. (2010) Systematic sequencing of renal carcinoma reveals inactivation of histone modifying genes. *Nature* 463:360–363.
6. Hughes CM, et al. (2004) Menin associates with a trithorax family histone methyltransferase complex and with the hoxc8 locus. *Mol Cell* 13:587–597.
7. Sellers WR, Kaelin WG, Jr. (1997) Role of the retinoblastoma protein in the pathogenesis of human cancer. *J Clin Oncol* 15:3301–3312.
8. Sellers WR, et al. (1998) Stable binding to E2F is not required for the retinoblastoma protein to activate transcription, promote differentiation, and suppress tumor cell growth. *Genes Dev* 12:95–106.
9. Benevolenskaya EV, Murray HL, Branton P, Young RA, Kaelin WG, Jr. (2005) Binding of pRB to the PHD protein RBP2 promotes cellular differentiation. *Mol Cell* 18: 623–635.
10. Zeng J, et al. (2010) The histone demethylase RBP2 Is overexpressed in gastric cancer and its inhibition triggers senescence of cancer cells. *Gastroenterology* 138:981–992.
11. Klose RJ, et al. (2007) The retinoblastoma binding protein RBP2 is an H3K4 demethylase. *Cell* 128:889–900.
12. Christensen J, et al. (2007) RBP2 belongs to a family of demethylases, specific for tri- and dimethylated lysine 4 on histone 3. *Cell* 128:1063–1076.
13. Iwase S, et al. (2007) The X-linked mental retardation gene SMCX/JARID1C defines a family of histone H3 lysine 4 demethylases. *Cell* 128:1077–1088.
14. Hayakawa T, et al. (2007) RBP2 is an MRG15 complex component and down-regulates intragenic histone H3 lysine 4 methylation. *Genes Cells* 12:811–826.
15. Marks PA, Breslow R (2007) Dimethyl sulfoxide to vorinostat: Development of this histone deacetylase inhibitor as an anticancer drug. *Nat Biotechnol* 25:84–90.
16. Kaminskas E, Farrell AT, Wang YC, Sridhara R, Pazdur R (2005) FDA drug approval summary: Azacitidine (5-azacytidine, Vidaza) for injectable suspension. *Oncologist* 10: 176–182.
17. Oki Y, Aoki E, Issa JP (2007) Decitabine—bedside to bench. *Crit Rev Oncol Hematol* 61: 140–152.
18. Clissold PM, Ponting CP (2001) JmjC: Cupin metalloenzyme-like domains in jumonji, hairless and phospholipase A2beta. *Trends Biochem Sci* 26:7–9.
19. Aravind L, Koonin EV (2001) The DNA-repair protein AlkB, EGL-9, and leprecan define new families of 2-oxoglutarate- and iron-dependent dioxygenases. *Genome Biol* 2: RESEARCH0007.
20. Ivan M, et al. (2002) Biochemical purification and pharmacological inhibition of a mammalian prolyl hydroxylase acting on hypoxia-inducible factor. *Proc Natl Acad Sci USA* 99:13459–13464.
21. Safran M, et al. (2006) Mouse model for noninvasive imaging of HIF prolyl hydroxylase activity: Assessment of an oral agent that stimulates erythropoietin production. *Proc Natl Acad Sci USA* 103:105–110.
22. Yokoyama A, et al. (2005) The menin tumor suppressor protein is an essential oncogenic cofactor for MLL-associated leukemogenesis. *Cell* 123:207–218.
23. Yokoyama A, et al. (2004) Leukemia proto-oncoprotein MLL forms a SET1-like histone methyltransferase complex with menin to regulate Hox gene expression. *Mol Cell Biol* 24:5639–5649.
24. Hayashi S, McMahon AP (2002) Efficient recombination in diverse tissues by a tamoxifen-inducible form of Cre: A tool for temporally regulated gene activation/inactivation in the mouse. *Dev Biol* 244:305–318.
25. Rangarajan A, Hong SJ, Gifford A, Weinberg RA (2004) Species- and cell type-specific requirements for cellular transformation. *Cancer Cell* 6:171–183.
26. Yates KE, Korbel GA, Shtutman M, Roninson IB, DiMaio D (2008) Repression of the SUMO-specific protease Senp1 induces p53-dependent premature senescence in normal human fibroblasts. *Aging Cell* 7:609–621.
27. Bernstein BE, et al. (2006) A bivalent chromatin structure marks key developmental genes in embryonic stem cells. *Cell* 125:315–326.
28. Subramanian A, et al. (2005) Gene set enrichment analysis: A knowledge-based approach for interpreting genome-wide expression profiles. *Proc Natl Acad Sci USA* 102: 15545–15550.
29. Shen X, et al. (2008) EZH1 mediates methylation on histone H3 lysine 27 and complements EZH2 in maintaining stem cell identity and executing pluripotency. *Mol Cell* 32:491–502.
30. Jacks T, et al. (1992) Effects of an Rb mutation in the mouse. *Nature* 359:295–300.
31. Clarke AR, et al. (1992) Requirement for a functional Rb-1 gene in murine development. *Nature* 359:328–330.
32. Lee EY, et al. (1992) Mice deficient for Rb are nonviable and show defects in neurogenesis and haematopoiesis. *Nature* 359:288–294.
33. de Bruin A, et al. (2003) Rb function in extraembryonic lineages suppresses apoptosis in the CNS of Rb-deficient mice. *Proc Natl Acad Sci USA* 100:6546–6551.
34. Wu L, et al. (2003) Extra-embryonic function of Rb is essential for embryonic development and viability. *Nature* 421:942–947.
35. Hu N, et al. (1994) Heterozygous Rb-1 delta 20/+mice are predisposed to tumors of the pituitary gland with a nearly complete penetrance. *Oncogene* 9:1021–1027.
36. Crabtree JS, et al. (2001) A mouse model of multiple endocrine neoplasia, type 1, develops multiple endocrine tumors. *Proc Natl Acad Sci USA* 98:1118–1123.
37. Crabtree JS, et al. (2003) Of mice and MEN1: Insulinomas in a conditional mouse knockout. *Mol Cell Biol* 23:6075–6085.
38. Herrera PL (2000) Adult insulin- and glucagon-producing cells differentiate from two independent cell lineages. *Development* 127:2317–2322.
39. Fontanière S, et al. (2006) Gene expression profiling in insulinomas of Men1 beta-cell mutant mice reveals early genetic and epigenetic events involved in pancreatic beta-cell tumorigenesis. *Endocr Relat Cancer* 13:1223–1236.
40. Brehm A, et al. (1998) Retinoblastoma protein recruits histone deacetylase to repress transcription. *Nature* 391:597–601.
41. Magnaghi-Jaulin L, et al. (1998) Retinoblastoma protein represses transcription by recruiting a histone deacetylase. *Nature* 391:601–605.
42. Luo RX, Postigo AA, Dean DC (1998) Rb interacts with histone deacetylase to repress transcription. *Cell* 92:463–473.
43. Dunaief JL, et al. (1994) The retinoblastoma protein and BRG1 form a complex and cooperate to induce cell cycle arrest. *Cell* 79:119–130.
44. Strober BE, Dunaief JL, Guha, Goff SP (1996) Functional interactions between the hBRM/hBRG1 transcriptional activators and the pRB family of proteins. *Mol Cell Biol* 16:1576–1583.
45. Nielsen SJ, et al. (2001) Rb targets histone H3 methylation and HP1 to promoters. *Nature* 412:561–565.
46. Kim KC, Geng L, Huang S (2003) Inactivation of a histone methyltransferase by mutations in human cancers. *Cancer Res* 63:7619–7623.
47. Gonzalo S, et al. (2005) Role of the RB1 family in stabilizing histone methylation at constitutive heterochromatin. *Nat Cell Biol* 7:420–428.
48. Robertson KD, et al. (2000) DNMT1 forms a complex with Rb, E2F1 and HDAC1 and represses transcription from E2F-responsive promoters. *Nat Genet* 25:338–342.
49. Lopez-Bigas N, et al. (2008) Genome-wide analysis of the H3K4 histone demethylase RBP2 reveals a transcriptional program controlling differentiation. *Mol Cell* 31: 520–530.
50. Cloos PA, Christensen J, Agger K, Helin K (2008) Erasing the methyl mark: Histone demethylases at the center of cellular differentiation and disease. *Genes Dev* 22: 1115–1140.
51. Martin C, Zhang Y (2005) The diverse functions of histone lysine methylation. *Nat Rev Mol Cell Biol* 6:838–849.
52. Milne TA, et al. (2002) MLL targets SET domain methyltransferase activity to Hox gene promoters. *Mol Cell* 10:1107–1117.
53. Nakamura T, et al. (2002) ALL-1 is a histone methyltransferase that assembles a supercomplex of proteins involved in transcriptional regulation. *Mol Cell* 10:1119–1128.

54. Varambally S, et al. (2002) The polycomb group protein EZH2 is involved in progression of prostate cancer. *Nature* 419:624–629.
55. van Haaften G, et al. (2009) Somatic mutations of the histone H3K27 demethylase gene UTX in human cancer. *Nat Genet* 41:521–523.
56. Northcott PA, et al. (2009) Multiple recurrent genetic events converge on control of histone lysine methylation in medulloblastoma. *Nat Genet* 41:465–472.
57. Blair LP, Cao J, Zou MR, Sayegh J, Yan Q (2011) Epigenetic regulation by lysine demethylase 5 (KDM5) enzymes in cancer. *Cancers (Basel)* 3:1383–1404.
58. van Zutven LJ, et al. (2006) Identification of NUP98 abnormalities in acute leukemia: JARID1A (12p13) as a new partner gene. *Genes Chromosomes Cancer* 45:437–446.
59. Wang GG, et al. (2009) Haematopoietic malignancies caused by dysregulation of a chromatin-binding PHD finger. *Nature* 459:847–851.
60. Sharma SV, et al. (2010) A chromatin-mediated reversible drug-tolerant state in cancer cell subpopulations. *Cell* 141:69–80.
61. Lu PJ, et al. (1999) A novel gene (PLU-1) containing highly conserved putative DNA/chromatin binding motifs is specifically up-regulated in breast cancer. *J Biol Chem* 274:15633–15645.
62. Xiang Y, et al. (2007) JARID1B is a histone H3 lysine 4 demethylase up-regulated in prostate cancer. *Proc Natl Acad Sci USA* 104:19226–19231.
63. Yamane K, et al. (2007) PLU-1 is an H3K4 demethylase involved in transcriptional repression and breast cancer cell proliferation. *Mol Cell* 25:801–812.
64. Roesch A, et al. (2010) A temporarily distinct subpopulation of slow-cycling melanoma cells is required for continuous tumor growth. *Cell* 141:583–594.
65. Dey BK, et al. (2008) The histone demethylase KDM5b/JARID1b plays a role in cell fate decisions by blocking terminal differentiation. *Mol Cell Biol* 28:5312–5327.
66. Harbour JW, et al. (1988) Abnormalities in structure and expression of the human retinoblastoma gene in SCLC. *Science* 241:353–357.
67. Loffler KA, et al. (2007) Lack of augmentation of tumor spectrum or severity in dual heterozygous Men1 and Rb1 knockout mice. *Oncogene* 26:4009–4017.
68. Matoso A, Zhou Z, Hayama R, Flesken-Nikitin A, Nikitin AY (2008) Cell lineage-specific interactions between Men1 and Rb in neuroendocrine neoplasia. *Carcinogenesis* 29: 620–628.
69. Minamishima YA, et al. (2008) Somatic inactivation of the PHD2 prolyl hydroxylase causes polycythemia and congestive heart failure. *Blood* 111:3236–3244.
70. Li C, Wong WH (2001) Model-based analysis of oligonucleotide arrays: Model validation, design issues and standard error application. *Genome Biol* 2: RESEARCH0032.
71. Kulkarni RN, et al. (1997) Leptin rapidly suppresses insulin release from insulinoma cells, rat and human islets and, in vivo, in mice. *J Clin Invest* 100:2729–2736.